

Experimental determination of the full Landau potential of bent-core doped ferroelectric liquid crystals

P. Archer and I. Dierking*

School of Physics and Astronomy, University of Manchester, Schuster Building, Oxford Road, Manchester M13 9PL, United Kingdom

(Received 14 June 2005; revised manuscript received 3 August 2005; published 28 October 2005)

The full Landau potential of a ferroelectric liquid crystal, doped with two different bent-core molecules at varying concentration, was determined experimentally. Using a multicurve fitting procedure, temperature and electric field dependent tilt angle and polarization measurements were analyzed according to the generalized Landau model of ferroelectric liquid crystals. From this analysis the three Landau coefficients as well as the polarization-tilt coupling parameters were obtained as a function of dopant concentration. It is shown that the two most varied parameters are those of the first Landau coefficient and the (chiral) linear polarization-tilt coupling constant. The results quantitatively verify the chiral induction capability of nonchiral bent-core shaped dopants and an observed increase in the electroclinic effect with increasing dopant concentration.

DOI: 10.1103/PhysRevE.72.041713

PACS number(s): 64.70.Md, 77.80.Bh, 77.84.Nh

I. INTRODUCTION

Ferroelectric liquid crystals [1–3] have been the subject of extensive investigations since Meyer *et al.* [4] first demonstrated that a tilted smectic liquid crystal composed of chiral molecules can exhibit a spontaneous polarization \mathbf{P}_S . The most prominent manifestation of such behavior is found in the helielectric SmC^* phase. On application of an electric field the spontaneous polarization aligns along the field direction. This realignment can be exploited to switch between two states on application of an ac electric field. It was the discovery of the surface stabilized geometry by Clark and Lagerwall [5] that largely promoted the study of helielectric liquid crystals and made them of key technological importance. In the simplest case, liquid crystals can be viewed as long “rodlike” molecules. In the SmA^* phase these molecules form layers in addition to the purely orientational order of the nematic phase, such that the director, \mathbf{n} , lies parallel to the smectic layer normal. In the low-temperature SmC^* phase the director is inclined at an angle Θ , the tilt angle, with respect to the layer normal. In thin surface stabilized devices with cell gaps smaller than the pitch of the intrinsic helical superstructure of the SmC^* phase, the helix is suppressed and ferroelectric behavior is observed [5].

Subsequent to the discovery of ferroelectric liquid crystals much work has been undertaken to develop a theoretical basis of the second order phase transition from the paraelectric SmA^* phase to the ferroelectric SmC^* phase. The bulk of this work is based on the general Landau theory for phase transitions. For both achiral and chiral systems, the primary order parameter of the transition from the nontilted $\text{SmA}^{(*)}$ to the tilted $\text{SmC}^{(*)}$ phase is generally considered to be the scalar parameter of the tilt angle, Θ . Nevertheless, the basic description is in very close analogy to ferromagnetic systems, where the magnetization \mathbf{M} is taken as the primary order parameter. The reason for the choice of Θ instead of \mathbf{P}_S

as the primary order parameter for the smectic A to C liquid crystal transition is the fact that a comprehensive theory should describe both achiral and chiral systems. As a spontaneous polarization can only occur in a chiral system, P_S is considered as a secondary order parameter of the SmA^* to SmC^* transition, which is coupled to the tilt angle Θ .

The classic Landau theory expands the free enthalpy density difference $g - g_0$ between the high-temperature SmA and the low-temperature SmC phase in even powers with respect to the (achiral) order parameter Θ as

$$g - g_0 = \frac{1}{2}a(T - T_C)\Theta^2 + \frac{1}{4}b\Theta^4 + \frac{1}{6}c\Theta^6 + \dots \quad (1)$$

The coefficient $a = 1/2a(T - T_C)$ is linearly dependent on temperature, reversing its sign as the phase transition is crossed at T_C . Further it is $b > 0$ for a second order transition ($b < 0$ for a first order transition) and $c > 0$ [6,7]. The expansion is generally cut off after the third term in Θ , with the Θ^6 term having been shown to be of importance in the description of the potential [7].

Considering chiral materials the occurrence of a local spontaneous polarization, as well as the formation of a helical superstructure with wave-vector q_0 , have to be taken into account [8]. In the case of the surface stabilized geometry the helical pitch is infinite, i.e., $q_0 = 0$. This condition was fulfilled in all the experiments presented below. The total polarization P is accounted for by (i) a dipolar ordering term $P^2/2\varepsilon_0\chi_0$, with χ_0 being the dielectric susceptibility at large frequencies along the electric field direction, and (ii) a bilinear coupling term between tilt Θ and polarization P is added, $-C\Theta P$, which describes electroclinic (piezoelectric) effects [9]. We note that the bilinear coupling coefficient C is *chiral* in nature:

$$g - g_0 = \frac{1}{2}a(T - T_C^*)\Theta^2 + \frac{1}{4}b\Theta^4 + \frac{1}{6}c\Theta^6 + \frac{P^2}{2\varepsilon_0\chi_0} - C\Theta P. \quad (2)$$

Equation (2) implies a linear dependence of polarization with tilt, a relation, which is generally in contradiction to experi-

*Author to whom correspondence should be addressed. Electronic address: ingo.dierking@manchester.ac.uk

mental findings, especially for large tilt angles at temperatures well below the transition temperature. Within the generalized Landau theory of ferroelectric liquid crystals [10,11] these deviations are accounted for by quadrupolar ordering, leading to a biquadratic coupling term $-\Omega P^2 \Theta^2/2$, with Ω being the quadrupolar coupling coefficient, which is *achiral* in nature. The difference in free enthalpy density within the generalized Landau model is then given by

$$g - g_0 = \frac{1}{2} \alpha (T - T_C^*) \Theta^2 + \frac{1}{4} b \Theta^4 + \frac{1}{6} c \Theta^6 + \frac{P^2}{2 \varepsilon_0 \chi_0} - C \Theta P - \frac{\Omega P^2 \Theta^2}{2}, \quad (3)$$

where we neglect a term $1/4 \eta P^4$ ($\eta > 0$), which was originally added for stability reasons, but which has no physical justification. On electric field application of amplitude E the free enthalpy density is finally given by

$$g - g_0 = \frac{1}{2} \alpha (T - T_C^*) \Theta^2 + \frac{1}{4} b \Theta^4 + \frac{1}{6} c \Theta^6 + \frac{P^2}{2 \varepsilon_0 \chi_0} - C \Theta P - \frac{\Omega P^2 \Theta^2}{2} - PE. \quad (4)$$

This description neglects any detailed surface interactions besides the unwinding of the helical superstructure ($q_0=0$), as well as flexoelectric effects. For the analysis presented below, this is justified, because experiments were carried out at constant cell gap in the bookshelf-geometry, i.e., possible small surface interactions would be equivalent for all samples and spatial variations of the director field are absent.

Prior to the electro-optic investigations of Giesselmann *et al.* [12,13], only a few attempts have been made to experimentally obtain a quantitative determination of the Landau coefficients of ferroelectric liquid crystals. The latter were mainly based on calorimetric measurements [14–16] and the electroclinic effect [17]. In this investigation we determine the full Landau potential of a ferroelectric liquid crystal, doped by different mesogenic and nonmesogenic achiral bent-core molecules [18–20] with varying bent-core angle, and additionally varying their concentrations, in order to elucidate the effects of achiral dopants on the individual, chiral, and nonchiral coefficients of the general Landau expansion.

II. EXPERIMENTAL METHODOLOGY

Minimization of the Landau free energy density [Eq. (4)] with respect to the total polarization gives [13,21]

$$P = \frac{C \Theta + E}{\frac{1}{\varepsilon_0 \chi_0} - \Omega \Theta^2}. \quad (5)$$

Thus, from the variation of the temperature dependence of the polarization with that of the tilt angle, C , χ_0 and Ω can be determined by use of a simultaneous multivariate fitting procedure with respect to the electric field dependence. Minimization of the free energy density [Eq. (4)] with respect to the tilt angle and rearranging terms, leads to the expression [13,21]:

$$T(\Theta, E) = T_C^* - \frac{1}{\alpha} \left[b \Theta^2 + c \Theta^4 - \frac{(C \Theta + E) \left(\frac{C}{\varepsilon_0 \chi_0} + \Omega \Theta E \right)}{\Theta \left(\frac{1}{\varepsilon_0 \chi_0} - \Omega \Theta^2 \right)} \right]. \quad (6)$$

Equation (6) does not directly describe the temperature and electric field dependence of the tilt angle, but rather the inverse relationship, the temperature as a function of tilt and field. A respective representation and use of the previously determined parameters C , χ_0 , and Ω then allows the values of α , b , c , and T_C^* to be determined from the second set of simultaneously fitted curves, $\Theta(T, E)$.

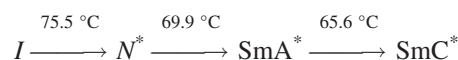
Substituting the polarization [Eq. (5)] into the generalized Landau expansion [Eq. (4)], the difference in free energy density between the high temperature SmA^* and the low temperature SmC^* phase is given by

$$g - g_0 = \frac{1}{2} \alpha (T - T_C^*) \Theta^2 + \frac{1}{4} b \Theta^4 + \frac{1}{6} c \Theta^6 - \frac{1}{2} \frac{(C \Theta + E)^2}{\left(\frac{1}{\varepsilon_0 \chi_0} - \Omega \Theta^2 \right)}. \quad (7)$$

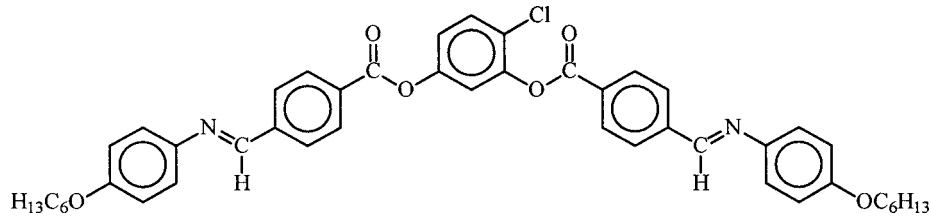
With all parameters known, Eq. (7) can be employed to visualize the full Landau potential on a quantitative basis at varying external conditions, i.e., temperature, electric field, and dopant concentration. Especially, the temperature dependence of the zero electric field tilt angle can be calculated, a quantity that is otherwise not accessible from electro-optic experiments. The electric field induced electroclinic tilt, $\delta \Theta$, can then be deduced on both sides of the transition by subtracting the extrapolated zero field tilt, Θ_0 , from the measured tilt angles, Θ_m :

$$\delta \Theta = \Theta_m - \Theta_0. \quad (8)$$

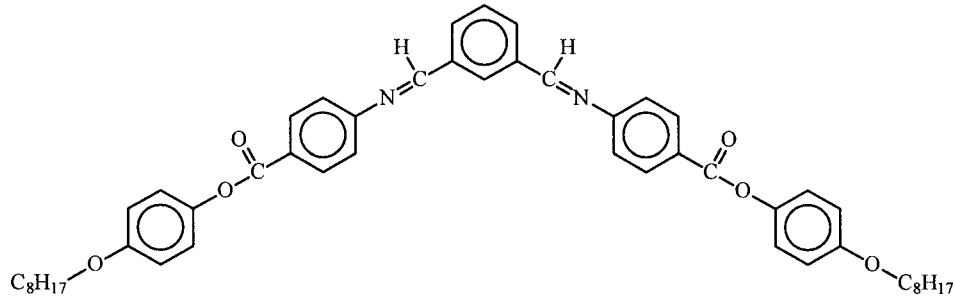
The ferroelectric liquid crystal matrix employed is the commercial mixture FELIX M4851/050 from Clariant, Wiesbaden, Germany whose phase sequence on cooling was determined to:



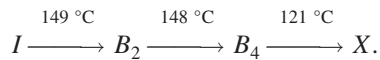
The liquid crystal was doped with various concentrations of two different bent-core shaped molecules denoted here as “859” and “HXVIII.” The first bent-core molecule, “859”:



is nonmesogenic with an isotropic to crystalline transition at 138 °C on cooling. The second bent-core molecule, “HXVIII”:



is mesogenic with phase sequence on cooling of



Doping the commercial FLC mixture with either of the bent-core molecules resulted in decreased phase transition temperatures with increasing dopant concentration. This however does not influence the analysis shown below, as T_{C^*} is one of the fitting parameters. The bend angles, i.e., the angle between the two molecular arms, and the arm lengths of the dopant molecules was determined by molecular modeling with HYPERCHEM 7.5. The bend angles of the molecules were 144° and 119° and the arm lengths were 21.7 and 21.1 Å for “859” and “HXVIII,” respectively. Mixtures were prepared for dopant concentrations up to 2.5% by weight, and phase separation was observed for concentrations larger than 3%.

The mixtures were capillary filled into 4 μm thick sandwich cells consisting of a transparent ITO electrode area with antiparallel rubbed polyimide alignment layers and cells were sufficiently thin to suppress the helical superstructure of the SmC^* phase in all cases. The electro-optic setup included a polarizing microscope (Leica DMLP) in conjunction with a Linkam hotstage (TDS600) and temperature controller (TP92) for relative accuracy within 0.1 K. Electric fields were applied by a function generator (Thurlby Thandar TGA1241) via a fixed-gain amplifier. For the tilt angle measurements a digital oscilloscope (Tektronix TDS3014B) was used to record the electro-optic response from a photodiode. Tilt angle measurements were carried out according to a method described in [22], with a square wave electric field applied to the sample while recording the corresponding light transmission intensities of the polarization up and down states for various rotation angles φ of the sandwich cell between crossed polarizers. The obtained data is then simultaneously fitted to two $\sin^2 \varphi$ curves and the tilt angle, Θ , determined from the phase difference between the two

curves: $\Delta\varphi=2\Theta$. Polarization measurements were performed using the well-established triangular wave method [23]. A triangular wave is applied to the sample and the corresponding current response curve recorded. The total polarization is the integrated value of the whole reversal current, not only the peak as for the case of the spontaneous polarization. Prior to integration the ohmic contribution was subtracted.

III. RESULTS AND DISCUSSION

Through small angle x-ray analysis (Daresbury synchrotron source, station 2.1), the layer spacing in the SmA^* phase of the FLC host was measured to be 29.9 Å, which is significantly larger than the arm lengths of either the “859” or “HXVIII” molecules, with 21.7 and 21.1 Å, respectively. Consequently, and in contrast to the observation of induced antiferroelectric phases [24–26], where the bent-core dopant arm length matched that of the hosts layer spacing, no such behavior was observed in this study.

Figure 1(a) shows the tilt angle variation with dopant concentration at a reduced temperature $T_{C^*}-T=33.5$ K, i.e., close to room temperature in the SmC^* phase. A decrease in the tilt angle with increasing bent-core concentration was observed. A decrease in the spontaneous polarization is associated with the decrease in tilt angle [Fig. 1(b)], as also previously reported [24]. “859,” the dopant molecule with the larger bend angle, was observed to cause a slightly larger decrease of the tilt angle as compared to “HXVIII.”

To illustrate the employed method of parameter determination of the generalized Landau expansion, sample data for the undoped matrix FLC is shown for polarization P versus tilt angle Θ and temperature T versus tilt angle Θ in Figs. 2(a) and 2(b), respectively, across the SmA^* - SmC^* transition. Figure 2 depicts data for the pure FLC FELIX M4851/050, but it should be noted that equivalent sets of curves were obtained for all systems at varying concentrations of

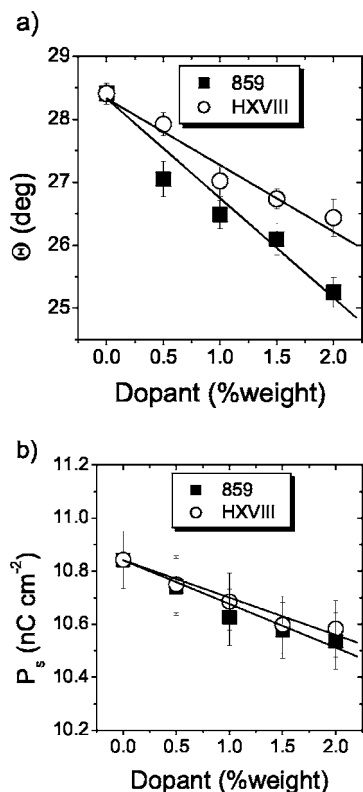


FIG. 1. (a) Tilt angle Θ and (b) spontaneous polarization P_S as a function of bent-core dopant concentration at reduced temperature of $T - T_{C^*} = -33.5$ K (\approx room temperature in the SmC* phase) for the “859” (closed squares) and “HXVIII” (open circles) doped samples. Lines are a guide to the eye.

both dopants. In all cases the threshold field was much smaller than $1 \text{ V } \mu\text{m}^{-1}$. Parameters χ_0 , C , and Ω are determined by *simultaneously* fitting all of the $P(\Theta, E)$ -data (all symbols) displayed in Fig. 2(a) to Eq. (5). The result is shown as solid lines, very well describing all five $P(\Theta)$ -curves at different applied electric field amplitudes E with only one parameter set (χ_0, C, Ω). χ_0 is proportional to the constant polarization steps at small tilt angles for constant increase of field amplitude, C is determined by the initial slope $dP/d\Theta$ for small tilt angles and Ω by the deviation of the linear polarization-tilt relationship at large tilt angles. Figure 2(b) illustrates the respective *simultaneous* fit (solid lines) of the experimentally determined temperature and field dependent tilt angle $\Theta(T, E)$ -data (all symbols), or as given here in the representation of Eq. (6), $T(\Theta, E)$. From this the parameter set α, b, c , and T_{C^*} is inferred, with the previously determined values of χ_0, C , and Ω kept constant. The extrapolated zero-field tilt angle $\Theta_0(T)$ is additionally shown in Fig. 2(b) as the dotted line. Already from Fig. 2(b) the intrinsically chiral electroclinic effect (solid lines and symbols as compared to the dotted line for zero-field), which is related to the parameters α and C , is clearly apparent. It will be discussed in more detail below, especially with respect to bent-core dopant concentration.

Equivalent sets of curves as depicted in Figs. 2(a) and 2(b) were also obtained for all of the bent-core doped samples. As we cannot present all original data involved in

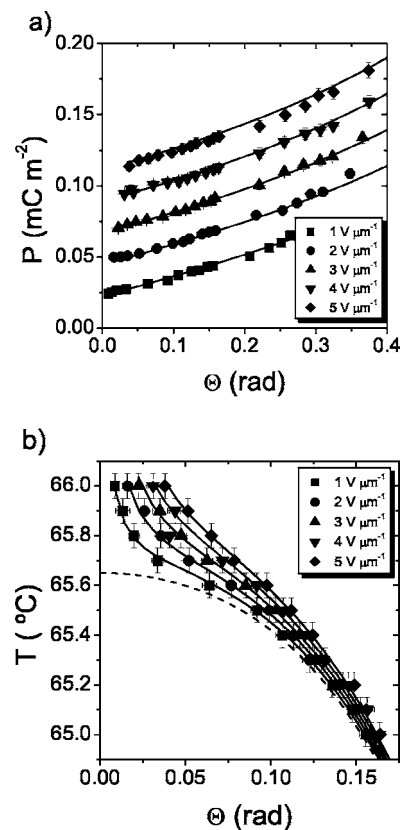


FIG. 2. Exemplary demonstration of the multicurve fitting procedures employed to determine the full Landau potential. Data is shown for the neat ferroelectric liquid crystal host material FELIX M4851/050, but it should be noted that all bent-core doped systems displayed equivalent behavior. (a) Experimental polarization data $P(\Theta, E)$ (symbols) and simultaneous best fits to Eq. (5) (solid lines) to determine the parameters χ_0, C , and Ω . (b) Experimental tilt angle data $\Theta(T, E)$ (symbols) and simultaneous best fits to Eq. (6) (solid lines) to determine α, b, c , and T_{C^*} . The dashed line denotes the calculated temperature dependence of the tilt angle at zero electric field.

the study, because this would imply another eight figures very similar to both parts of those of Fig. 2, we restrict ourselves to give exemplary concentration dependent data for the “859” dopant at a field amplitude of $4 \text{ V } \mu\text{m}^{-1}$. The relation between polarization P and tilt angle Θ is depicted in Fig. 3(a), for increasing concentration of the bent-core dopant. Solid lines represent the original fit to Eq. (5) using all temperature and field dependent data. The initial slope, $dP/d\Theta$ at small tilt angles, which determines the value of the bilinear (piezoelectric) coupling term C is found to increase with increasing dopant concentration. The corresponding temperature dependence of the tilt angle is shown in Fig. 3(b), where reduced temperatures $T - T_{C^*}$ have been used, because the SmA*-SmC* phase transition temperature slightly changes with increasing dopant concentration. Solid lines represent the original fit to Eq. (6) using all temperature and field dependent data. The steepness of the curves decreases with increasing bent-core dopant concentration, illustrating a decrease of the α -term. Each single set of Landau constants, for each concentration of the two dopants, is thus

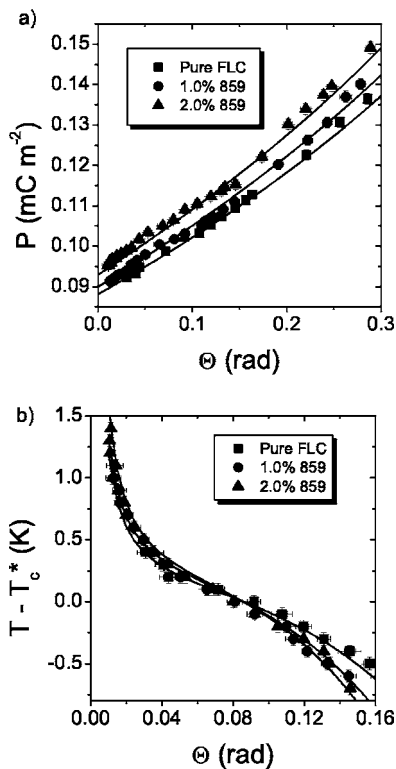


FIG. 3. Exemplary data of (a) $P(\Theta)$ and (b) $T(\Theta)$ at varying concentration of the “859” bent-core dopant molecule at a fixed electric field amplitude of $E=4 \text{ V } \mu\text{m}^{-1}$. Solid lines represent the fits obtained from Eqs. (5) and (6), respectively, using all temperature and field dependent data for each concentration. The data implies an increase of the bilinear (piezoelectric) coupling constant C and a decrease of the α -term for increasing dopant concentration.

determined by approximately 150 temperature and electric field dependent measurements.

Figure 4 summarizes the dependence of all parameters of the generalized Landau model, α , b , c , χ_0 , C , and Ω , determined as a function of the dopant concentration for both bent-core molecules, “859” (closed squares) and “HXVIII” (open circles). The coefficients determined with the highest confidence are those of the first Landau constant α and of the linear polarization-tilt coupling C , because these are the ones that lead to the largest change in electro-optic behavior across the second order $\text{SmA}^*-\text{SmC}^*$ transition. The first Landau coefficient α clearly decreases with increasing dopant concentration, as depicted in Fig. 4(a). This implies a broadening of the potential at the phase transition and is supported by the experimentally observed increase of the electroclinic effect for increasing bent-core molecule concentration.

The second Landau coefficient, b [Fig. 4(b)], is related to the order of the phase transition. We determine $b > 0$ in all cases, thus indicating a second order transition, which is not altered as the concentration of the bent-core dopant is increased. Within experimental error the Landau coefficient b is constant, $b=(1 \pm 0.2) \times 10^6 \text{ J m}^{-3}$, independent of dopant concentration as well as the specific molecular constitution of the dopant material. The third Landau coefficient, c , is not very well determined from the analysis procedure outlined

above. It mainly influences the steepness of the potential at large tilt angles, which means that only minute changes in Θ can imply a relatively large change in c . The c -coefficients depicted in Fig. 4(c) should thus be taken to be correct within a factor of about 2, and suggested trends should not be considered of being of significant relevance. Within the scope of this analysis the third Landau coefficient can be considered to be in the order of $c=(2 \pm 1) \times 10^7 \text{ J m}^{-3}$, and independent of the dopant’s molecular constitution and concentration within the limit of dopant solubility.

The dielectric susceptibility at high frequencies χ_0 remains largely unchanged for both of the bent-core doped mixtures [Fig. 4(d)], being basically independent of dopant constitution and concentration. The value obtained is $\chi_0 = 2.55 \pm 0.05$. This result can be understood by the only very small amount of added bent-core molecules, smaller than 3%, and dopants being of a comparable chemical constitution, thus similar molecular polarizability, as the FLC host material.

In contrast, the linear polarization-tilt coupling coefficient C clearly increases for increasing dopant concentration. Besides the Landau coefficient α , this is another parameter, which is very well defined through the analysis procedure, because it significantly determines the electro-optic behavior of the doped FLC matrix in the temperature region across the $\text{SmA}^*-\text{SmC}^*$ transition [Fig. 4(e)]. As the linear polarization-tilt coupling parameter is intrinsically chiral in nature, the observed increase in C with dopant concentration of an achiral bent-core dopant implies a *chiral* induction capability of *achiral* bent-core molecules. This significant result will be discussed in more detail below.

Finally, the biquadratic coupling constant Ω is related to the quadrupolar order of the system. In first approximation, liquid crystal molecules are often considered to be either of ellipsoidal or cylindrical shape. However, deviations from the cylindrical molecular shape towards a lathlike or brick-like structure need to be accounted for by quadrupolar ordering. In the Landau description of FLCs this is quantified by the biquadratic polarization-tilt coupling coefficient, Ω . The effects of quadrupolar ordering are generally of comparably small magnitude. Consequently, the determination of the dopant concentration dependence of the biquadratic polarization-tilt coupling parameter has to be taken with some caution. For both of the bent-core dopants investigated at relatively small concentrations, Ω should practically be considered as constant within the limits of uncertainty, independent of dopant concentration and constitution [Fig. 4(f)], at $\Omega=(3.5 \pm 0.5) \times 10^{10} \text{ V m C}^{-1}$.

The determined constants are in accordance with coefficients determined on undoped commercial ferroelectric liquid crystal mixtures [13,21] and are of the same order of magnitude as some neat FLCs [14–17]. It should also be noted that the $\text{SmA}^*-\text{SmC}^*$ phase transition temperatures observed by polarizing microscopy are absolutely consistent with those obtained by the fitting procedure. Due to the rather small spontaneous polarization of the host material, the transition temperatures of the hypothetical achiral (T_c) and the chiral materials (T_{c^*}) are practically equivalent. Their difference is governed by the ratio $\epsilon_0 \chi_0 C^2 / \alpha$ which in the present case yields approximately 0.02 K.

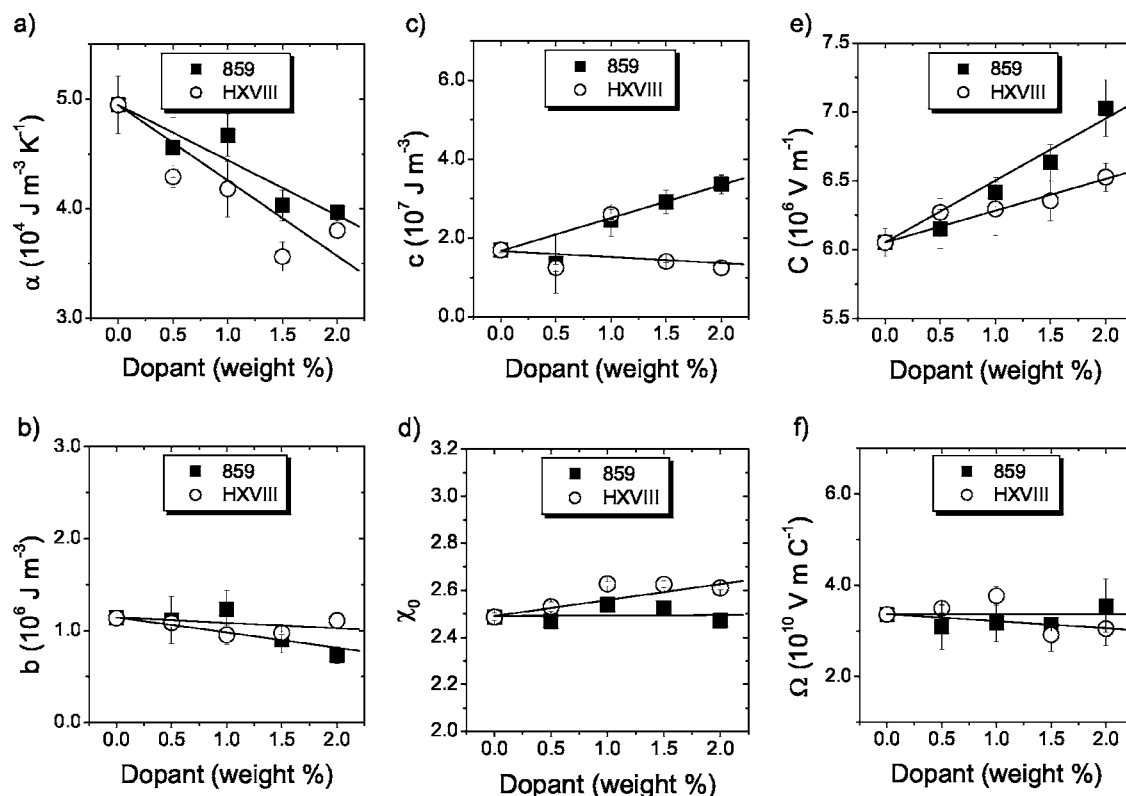


FIG. 4. Dependence of all parameters of the generalized Landau potential on bent core dopant concentration for the molecules “859” (closed squares) and “HXVIII” (open circles). (a) First Landau coefficient, α , (b) second Landau coefficient, b , (c) third Landau coefficient, c , (d) dielectric constant at high frequencies, χ_0 , (e) bilinear polarization-tilt coupling coefficient C , and (f) biquadratic polarization-tilt coupling coefficient Ω . Lines are a guide to the eye; for a detailed discussion see the text.

Having determined the full set of material parameters of the generalized Landau expansion, the free energy density, $g - g_0$, can be studied in detail using Eq. (7). Note that this can be done on a real, *quantitative* basis, relating to the actual materials under investigation. For illustration, the temperature and electric field dependence of the potential is discussed for the pure FELIX M4851/050 matrix in Fig. 5, noting that equivalent behavior is observed for all doped systems as well. Figure 5(a) depicts the temperature evolution of the potential across the SmA^* to SmC^* transition at zero electric field. In the SmA^* phase, i.e., for reduced temperatures $T - T_{C^*} > 0$, the potential has a single minimum at $\Theta = 0$, corresponding to the fact that the director is parallel to the smectic layer normal. Directly at the SmA^* - SmC^* phase transition ($T = T_{C^*}$) the potential broadens considerably [Fig. 5(a), solid line]. This makes it easy for the director to deviate from the $\Theta = 0$ position under small electric fields, accounting for the fact that the electroclinic effect is largest directly at the transition. For temperatures $T - T_{C^*} < 0$, i.e., in the SmC^* phase, two potential minima are observed for $\pm\Theta \neq 0$, corresponding to the two possible tilt positions in the surface stabilized state. The potential wells deepen for decreasing temperature, in accordance with the decrease of the electroclinic effect well below the transition. At the same time the potential minima move further apart for decreasing temperature, consistent with an increase of tilt angle. Figure 5(b) shows the evolution of the potential at $T = T_{C^*}$ for increasing electric dc field amplitude. The potential is skewed to one

side and develops a minimum at nonzero tilt angle, which reflects the electroclinic effect. Further, the potentials minimum position shifts to larger tilt angles for increasing electric field, in accordance with the expected behavior of the electroclinic effect. The determined potentials for temperature and electric field variation (Figs. 5) qualitatively conform with the generally expected behavior: they explain the appearance and increase of the tilt angle with decreasing temperature below the SmA^* - SmC^* transition, as well as the temperature and electric field dependence of the electroclinic effect in both the paraelectric SmA^* and the ferroelectric SmC^* phase. In addition, the accessibility of the potential $g - g_0$ allows predictions of all of the quantities mentioned above on a *quantitative* basis for *all* temperatures and electric fields, thus also a complete electro-optic description of the system.

In the following we discuss the quantitative influence of bent-core dopant concentration and constitution on the potential. Figure 6 depicts potentials at $T - T_{C^*} = -1 \text{ K}$ in the SmC^* phase just below the transition temperature at zero electric field. In Fig. 6(a) the variation of the potential with increasing bent-core dopant “859” concentration is shown for the pure matrix and selected concentrations. For reasons of clarity, potentials are not shown for all concentrations investigated. It is apparent that the minimum of the potential becomes shallower with increasing dopant concentration. This implies a smaller threshold voltage for the ferroelectric switching process for increasing dopant concentration. At the same time the angular difference between the two potential

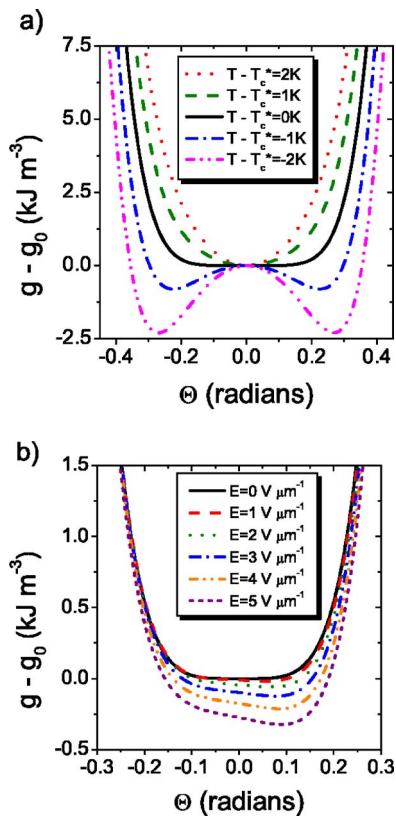


FIG. 5. (Color online) Exemplary calculated free enthalpy density difference, $g - g_0$ [Eq. (7)] for the neat ferroelectric liquid crystal host FELIX M4851/050 for (a) varied temperature across the SmA^* to SmC^* transition, i.e., $T - T_{C^*} > 0$, $T = T_{C^*}$, and $T - T_{C^*} < 0$ and (b) varied electric field amplitude E at reduced temperature $T = T_{C^*}$. The potentials calculated from the experimentally determined parameters (Fig. 4) are in accordance with the generally expected behavior: the occurrence of a tilt angle Θ at the SmA^* - SmC^* transition, increasing tilt angle with decreasing temperature, and the generally observed behavior of the electroclinic effect. Note that the potentials are given in quantitative units.

minima decreases with increasing dopant concentration, indicating a reduction in tilt angle, as it was also found from direct measurements [Fig. 1(a)]. Figure 6(b) compares the effect of the different bent-core dopants with varying bend angle, on the Landau potential at equal concentration of 2% by weight. For both dopants the potential minima are less deep than those of the pure matrix (solid line), but there seems to be no significant effect of the bent-core molecular constitution, i.e., the bend-angle, on the potential.

Figure 7 depicts a quantitative comparison of the potential for applied positive electric fields of $E = 5 \text{ V } \mu\text{m}^{-1}$, again at $T - T_{C^*} = -1 \text{ K}$ in the SmC^* phase. As expected, one of the tilt angle positions, the one with the deeper potential minimum, is preferred over the other. From Fig. 7(a) it is clear that the tilt angle decreases as compared to the pure FLC matrix, with increasing “859” dopant concentration, but again no significant difference is observed for the two dopants with varying bent-core angle at equal concentrations of 2% by weight [Fig. 7(b)].

If a comparison of the relative contributions of the different terms in the free energy density [Eq. 8] is made, it is

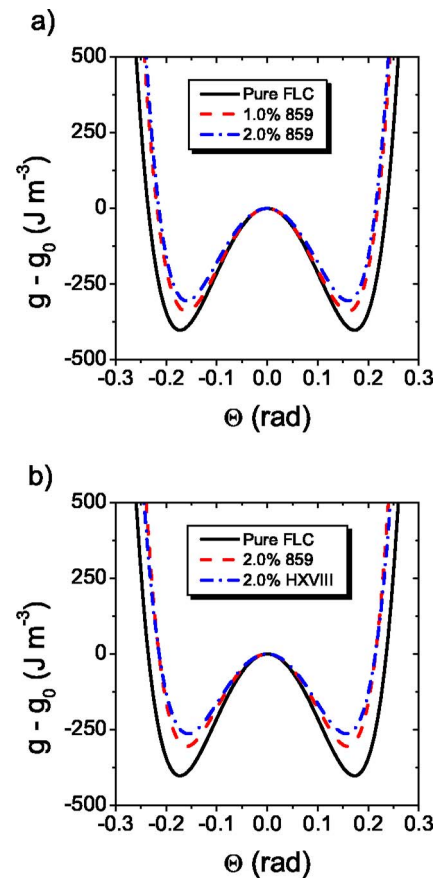


FIG. 6. (Color online) A quantitative comparison of the Landau potential in the SmC^* phase at reduced temperature $T - T_{C^*} = -1 \text{ K}$ and zero electric field for (a) varying bent-core dopant concentration and (b) varying bent-core molecular constitution at constant concentration with respect to the potential of the neat liquid crystal host (solid line).

found that in the vicinity of the transition the most significant influence is clearly that of the electric field dependent contribution, exemplifying the electroclinic effect (Fig. 7, for the pure FLC matrix; equivalent graphs are obtained for all bent-core doped systems investigated). Further below the phase transition the electric field contribution to the free energy density quickly becomes very small and the potential is dominated by the original Landau expansion of Eq. (1). Within this regime the α -term is the most important, while the b - and c -terms exhibit approximately equal influence at a level of about 10% of that of the α -term.

As mentioned above, the employed experimental method implies that the electroclinic effect can be studied on both sides of the SmA^* to SmC^* phase transition. This is only possible as the temperature dependence of the SmC^* tilt angle can be calculated for zero electric field conditions. The electroclinically induced tilt, $\delta\Theta$ of the SmA^* phase depends linearly on the applied electric field. Figure 8 exemplarily depicts the comparison of an analysis of $\delta\Theta(T, E)$ using the calculated coefficients (solid lines) with experimental data (symbols) for varying electric field for the 2% HXVIII doped FLC matrix. Note that Fig. 9 depicts the temperature dependence of the electroclinically induced tilt in both the SmA^*

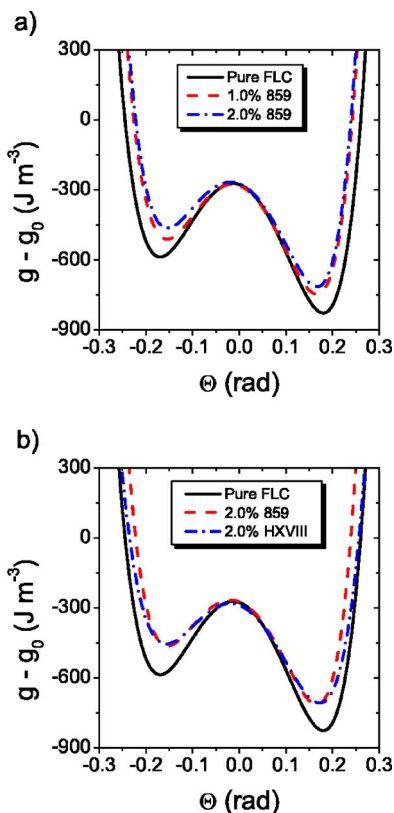


FIG. 7. (Color online) A quantitative comparison of the Landau potential in the SmC^* phase at reduced temperature $T - T_{C^*} = -1$ K and applied electric field amplitude of $E = 5 \text{ V } \mu\text{m}^{-1}$ for (a) varying bent-core concentration and (b) varying bent-core molecular constitution at constant concentration with respect to the potential of the neat liquid crystal host (solid line).

as well as the SmC^* phase. Again, comparable results were obtained for all concentrations of the two different bent-core dopants as well as the pure FLC matrix. The calculated behavior from the full Landau potential (solid lines) fits very well with the actually determined experimental data (symbols) for all electric fields applied.

Figure 10 shows the determined electroclinic coefficients $e^* = \chi_0 \epsilon_0 C / [\alpha(T - T_{C^*})]$ [2, Chap. 5.8] for both bent-core dopants “859” (squares) and “HXVIII” (circles) as a function of dopant concentration. e^* is obviously chiral in nature as it contains the bilinear coupling coefficient C . For both dopants the electroclinic coefficient linearly increases as a function of dopant concentration, giving unambiguous, quantitative evidence for the chiral induction capability of achiral bent-core molecules added to a chiral host material. An enhancement of chirality by achiral bent-core dopants had previously been observed through pitch measurements in the cholesteric [27] and the chiral SmC^* phase [28], as well as the induction of frustrated Blue Phases [29].

Such a behavior has very recently been predicted theoretically and through computer simulations [30,31]. The latter revealed several hundred conformations of a bent-core molecule with relatively similar energy, many of which were chiral. Introducing a chirality parameter, it was shown that equal distributions of left- and right-handed configurations

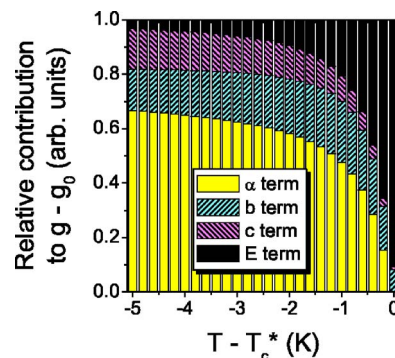


FIG. 8. (Color online) A quantitative comparison of the relative contributions of the Landau expansion terms to the potential of a ferroelectric liquid crystal, as exemplified for the neat FELIX M4851/050 host. Within the direct vicinity of the SmA^* - SmC^* phase transition ($T - T_{C^*}$ small and thus Θ being small), the electric coupling terms are most dominant. For lowering the temperature in the SmC^* phase the Landau terms become dominant. Note that an equivalent behavior is also observed for all of the bent-core doped systems.

are present, making the bent-core molecule achiral on a temporal average scale. Nevertheless, subjecting such a molecule to a chiral environment, as done in our experimental investigations, can bias this distribution of chiral configurations towards the handedness of the chiral host, either by shifting the symmetric distribution of chiral conformers or by making the distribution asymmetric about the zero value of the chirality parameter. The dopant bent-core molecule is made chiral on an average temporal basis by its chiral host and thus enhances the chiral properties of the doped system. At the same time the bent-core dopants also change the steric environment of the host molecules, influencing their rotational bias around the long molecular axes, which in turn influences the piezoelectric coupling. The overall effect is evidenced by the presented investigations, as the intrinsically chiral parameters of the bilinear polarization-tilt coupling term C [Fig. 4(e)] and thus also the electroclinic coefficient e^* [Fig. 10] clearly exhibit an increasing value for increasing

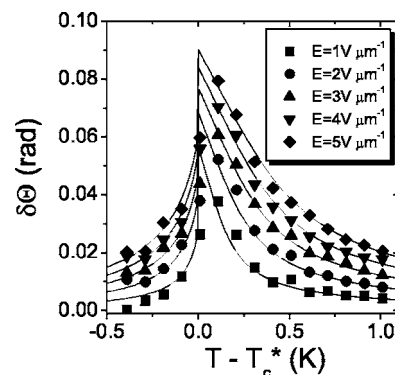


FIG. 9. Temperature and electric field dependence of the electroclinically induced tilt angle $\delta\Theta$ in both the SmA^* and the SmC^* phase for the 2% by weight HXVIII doped sample. The experimental results (symbols) are very well predicted by the calculations from the fully determined generalized Landau expansion (solid lines).

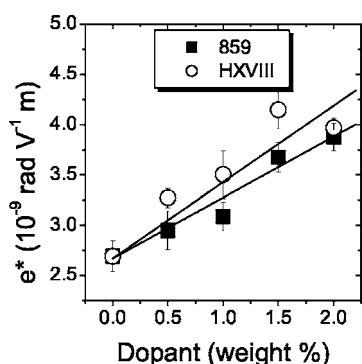


FIG. 10. Electroclinic coefficient e^* as a function of bent-core dopant concentration for the “859” (closed squares) and the “HXVIII” (open circles) molecules. In both cases the electroclinic coefficient linearly increases with increasing dopant concentration, giving quantitative evidence for the chiral induction capability of achiral bent-core dopants within a chiral host. The molecular constitution (bent angle) of the dopant does not seem to be of significant influence towards the observed behavior.

concentration of the achiral bent-core dopants. Within the limits of error, the increased chirality of the doped systems does not seem to be significantly correlated with the constitution of the dopant, i.e., the bent-angle between the two arms of the dopant molecule.

IV. CONCLUSIONS

The full Landau potential of bent-core doped ferroelectric liquid crystals was determined for different concentrations of

dopant molecules of varying molecular constitution. Two banana molecules with differing bend angles were doped into a commercial ferroelectric liquid crystal mixture and a multi-curve fitting procedure was employed on temperature and electric field dependent tilt angle and polarization data to determine all parameters of the generalized Landau expansion. The most significant effects were observed for the first Landau coefficient, α , and the bilinear coupling constant, C . For increasing dopant concentration of both bent-core molecules the α -term was found to decrease, giving evidence of an enhancement of the electroclinic effect. The bilinear coupling term between polarization and tilt was observed to increase with increasing dopant concentration, while other parameters were found to be largely unaffected within the margin of experimental error. The effect of bent-core dopants on the Landau potential of ferroelectric liquid crystals was discussed in detail on a quantitative basis. It was shown that the electroclinic coefficient, a quantity solely chiral in nature, is increased for increasing concentrations of achiral bent-core dopant molecules.

ACKNOWLEDGMENTS

We sincerely thank Rainer Wingen of Clariant, Wiesbaden, Germany, for providing the ferroelectric liquid crystal host mixture FELIX M4851/050 and Wolfgang Weissflog for the bent-core dopants. The provision of sandwich cells by Koen D'havé is gratefully acknowledged. This work was financially supported by the EPSRC through a DTA studentship for P.A. and the University of Manchester Research Support Fund.

- [1] J. W. Goodby, R. Blinc, N. A. Clark, S. T. Lagerwall, M. A. Osipov, S. A. Pikin, T. Sakurai, K. Yoshino, and B. Žekš, *Ferroelectric Liquid Crystals: Principles, Properties and Applications*, edited by G. Taylor (Gordon and Breach, Philadelphia, 1991), Sec. 7.
- [2] S. T. Lagerwall, *Ferroelectric and Antiferroelectric Liquid Crystals* (Wiley-VCH, Weinheim, 1999).
- [3] I. Mušević, R. Blinc, and B. Žekš, *The Physics of Ferroelectric and Antiferroelectric Liquid Crystals* (World Scientific, Singapore, 2000).
- [4] R. B. Meyer, L. Liébert, L. Strzelecki, and P. Keller, *J. Phys. (Paris), Lett.* **36**, L69 (1975).
- [5] N. A. Clark and S. T. Lagerwall, *Appl. Phys. Lett.* **36**, 899 (1980).
- [6] C. C. Huang and J. M. Viner, *Phys. Rev. A* **25**, 3385 (1982).
- [7] R. J. Birgeneau, C. W. Garland, A. R. Kortan, J. D. Litster, M. Meichle, B. M. Ocko, C. Rosenblatt, L. J. Yu, and J. Goodby, *Phys. Rev. A* **27**, 1251 (1983).
- [8] V. L. Indenbom, S. A. Pikin, and E. B. Loginov, *Sov. Phys. Crystallogr.* **21**, 632 (1976).
- [9] S. Garoff and R. B. Meyer, *Phys. Rev. Lett.* **38**, 848 (1977).
- [10] B. Žekš, *Mol. Cryst. Liq. Cryst.* **114**, 259 (1984).
- [11] T. Carlsson, B. Žekš, A. Levstik, C. Filipic, I. Levstik, and R. Blinc, *Phys. Rev. A* **36**, 1484 (1987).
- [12] F. Giesselmann and P. Zugenmaier, *Phys. Rev. E* **52**, 1762 (1995).
- [13] F. Giesselmann, A. Heimann, and P. Zugenmaier, *Ferroelectrics* **200**, 237 (1997).
- [14] T. Carlsson and I. Dahl, *Mol. Cryst. Liq. Cryst.* **95**, 373 (1983).
- [15] S. Dumrongrattana, C. C. Huang, G. Nounesis, S. C. Lien, and J. M. Viner, *Phys. Rev. A* **34**, 5010 (1986).
- [16] C. C. Huang and S. Dumrongrattana, *Phys. Rev. A* **34**, 5020 (1986).
- [17] Ch. Bahr, G. Heppke and B. Sabaschus, *Ferroelectrics* **84**, 103 (1988).
- [18] T. Niori, T. Sekine, J. Watanabe, T. Furukawa, and H. Takezoe, *J. Mater. Chem.* **6**, 1231 (1996).
- [19] D. R. Link, G. Natale, R. Shao, J. E. MacLennan, N. A. Clark, E. Körblova, and D. M. Walba, *Science* **278**, 1924 (1997).
- [20] G. Pelzl, S. Diele, and W. Weissflog, *Adv. Mater. (Weinheim, Ger.)* **11**, 707 (1999).
- [21] F. Giesselmann, Habilitation thesis, University of Clausthal, Germany, 1999.
- [22] C. Bahr and G. Heppke, *Liq. Cryst.* **2**, 825 (1987).
- [23] K. Miyasato, S. Abe, H. Takezoe, A. Fukuda, and E. Kuze, *Jpn. J. Appl. Phys., Part 2* **22**, L661 (1983).
- [24] E. Gorecka, M. Nakata, J. Mieczkowski, Y. Takanishi, K. Ish-

- ikawa, J. Watanabe, H. Takezoe, S. H. Eichhorn, and T. M. Swager, *Phys. Rev. Lett.* **85**, 2526 (2000).
- [25] P. K. Maiti, Y. Lansac, M. A. Glaser, and N. A. Clark, *Phys. Rev. Lett.* **88**, 065504 (2002).
- [26] K. Kishikawa, N. Muramatsu, S. Kohmoto, K. Yamaguchi, and M. Yamamoto, *Chem. Mater.* **15**, 3443 (2003).
- [27] J. Thisayukta, H. Niwano, H. Takezoe, and J. Watanabe, *J. Am. Chem. Soc.* **124**, 3354 (2002).
- [28] E. Gorecka, M. Čepič, J. Mieczkowski, M. Nakata, H. Takezoe, and B. Žekš, *Phys. Rev. E* **67**, 061704 (2003).
- [29] M. Nakata, Y. Takanishi, J. Watanabe, and H. Takezoe, *Phys. Rev. E* **68**, 041710 (2003).
- [30] D. J. Earl and M. R. Wilson, *J. Chem. Phys.* **119**, 10280 (2003).
- [31] D. J. Earl, M. A. Osipov, H. Takezoe, Y. Takanishi, and M. R. Wilson, *Phys. Rev. E* **71**, 021706 (2005).